AD NUMBER

AD254474

NEW LIMITATION CHANGE

TO

Approved for public release, distribution unlimited

FROM

Distribution authorized to U.S. Gov't. agencies and their contractors; Administrative/Operational Use; 28 Feb 1961. Other requests shall be referred to Office of Naval Research, Arlington, VA.

AUTHORITY

ONR ltr, 13 Sep 1977

UNIVERSITY OF PENNSYLVANIA

DEPARTMENT OF CHEMISTRY

PHILADELPHIA 4, PENNSYLVANIA

THE DETERMINATION OF THE COVERAGE ON NICKEL AND STEEL DURING ELECTROLYTIC HYDROGEN EVOLUTION

Technical Report No. 4
to
Office of Naval Research
Contract Nonr 551(22) NR 036-028

Principal Investigator - J. O'M. Bockris

Research Associate - M. A. V. Devanathan

February 28, 1961

Research Group in Electrochemistry and Electrometallurgy

The Department of Chemistry

The University of Pennsylvania

Philadelphia 4, Pennsylvania

THE DETERMINATION OF THE COVERAGE ON NICKEL AND STEEL DURING ELECTROLYTIC HYDROGEN EVOLUTION

SUMMARY

The galvanostatic double charging method previously developed in this project, has been applied to determine the coverage of nickel cathodes with adsorbed atomic hydrogen in 2 N sodium hydroxide solutions. Anodic current densities have been varied from 0.05 A cm^{-2} to 1.8 A cm^{-2}. The plateau indicating absence of readsorption was found between 0.6 and 1.8 A cm^{-2}, for a constant cathodic c.d. of 10^{-4} A cm^{-2}. The variation of the adsorbed hydrogen over cathodic c.d.'s ranging from 10^{-6} to 10^{-1} at a constant anodic c.d. of 1 A cm^{-2} have been calculated and the coverage calculated. The mechanism of the hydrogen evolution reaction has been elucidated with the aid of the coverage values obtained. It is shown that the rate determining step is discharge from a water molecules followed by rapid Tafel recombination. The rate constants for these processes and the rate constant for the ionisation, calculated with the extrapolated value of coverage for the reversible hydrogen electrode, have been determined. A modification of the Tafel equation which takes into account both coverage and ionisation is found to be in harmony with the results obtained.

A new method for the determination of coverage suitable for corrodible metals is described. This involves the measurement of the rate of permeation of hydrogen by electrochemical techniques which enhances the sensitivity of the method. The relevant diffusion theory suitable for this method is developed. A detailed analysis of the method shows that it can yield all parameters of significance in

hydrogen embrittlement studies, namely rate constants for transfer from surface to bulk and vice versa, the diffusion constant, and the quantity of hydrogen in the membrane.

The method has been tested on palladium and the diffusion constant evaluated by five different formulae from the rise and decay transients. Four of these formulae are original and the agreement of the results obtained by all five formulae confirms the validity of the equations derived. The method has been applied to nickel and steel. Preliminary data show that the coverage in alkaline solutions tends to 30% of that in acid solutions. Palladated steel membranes have also been studied. Evidence that the diffusion behaviour depends on past history of the specimen has been obtained.

THE DETERMINATION OF THE COVERAGE OF NICKEL AND STEEL DURING ELECTROLYTIC HYDROGEN EVOLUTION

INTRODUCTION

The main objectives of the present work is to devise methods whereby fractions of a monolayer of adsorbed atomic hydrogen covering cathodes during hydrogen evolution can be determined. The importance of the coverage factor θ lies in its application to the elucidation of the mechanism of the hydrogen evolution reaction. From the practical point of view, the determination of θ particularly on metals susceptible to hydrogen embrittlement is vital to the control and eventual elimination of the unpredictable behaviour of hydrogen embrittled materials. From among materials employed for structure fabrication iron, nickel and their alloys are those most susceptible to hydrogen embrittlement. The determination of θ on these substances especially in acid and other corrosive media can therefore be regarded as the principal objective.

STATUS OF METHODS AVAILABLE

A number of original methods[1,2] were proposed in ONR Technical Report 1, and a number of new ones outlined[3] in ONR Technical Report 3. Detailed consideration of the kinetic and thermodynamic parameters for a number of metals with respect to the applicability of the various methods were made and the conclusions are as follows:

1. Galvanostatic Double Charging Method:[1]

This method, which has been discussed in detail in Reports (1) and (2) can be used to determine θ in the following systems:

a. Noble metals in acid or alkaline media. Compensation curve unnecessary.

b. Transition metals in alkaline media.

c. Copper and silver in acid and alkaline media.

2. Anodic Potentiostatic Transient:[1]

Calculations show that while acid and alkaline media may be used in the following systems, there are restrictions in respect to θ and over-potential.

a. Nickel, $\theta_H \simeq 1$ η = .15 - 26 v $i_t < 10\ i_{an}$

b. Platinum, $\theta_H \simeq 0$ η = .15 to .48 v $i_t > 10\ i_{an}$

c. Gold, θ 0-1 η = .15 to .48 v $i_t > 10\ i_{an}$

3. Permeation Rate Method[3]

This method consists in estimating the quantity of hydrogen diffusing through a metal membrane one side of which is maintained at cathodic over potentials. Detailed consideration of the various possible mechanisms enables a functional dependence between the permeation rate and the cathodic current density to be derived for each mechanism. Knowledge of the mechanism from measurements of the throughput will give qualitatively the degree of coverage. This method is attractive from the point of view of embrittlement studies, as those metals which have high permeation rates would also be expected to show greater susceptibility to hydrogen embrittlement.

Experimental technique, however, is difficult, as the

quantities of hydrogen are minute and ionisation gauges or mass spectrometers have to be employed in conjunction with high vacuum systems in the 10^{-10} to 10^{-7} mm of Hg range.

4. Electrolyte Separation Factor

The electrolytic separation factor for hydrogen-deuterium or hydrogen-tritium is characteristic of the mechanism of hydrogen evolution reaction.[4] The separation factor can be calculated theoretically and confirm experimental results with metals, where the mechanism has been established by other methods. Measurement of the electrolytic separation factor would enable the identification of the mechanism and will therefore give qualitatively the coverage.

This method would be suited for iron in acid solution. Determinations have to be made at current densities in the range 10^{-2} to 10^{0} amp/cm^2 in order to collect appreciable amounts of hydrogen, which means that there must be indications that the mechanism does not change when below 10^{-2} amp/cm^2.

5. Determination of Pseudo-Capacitance

It has been shown that the pseudo-capacitance[5] gives a direct measure of the degree of coverage of an electrode. The pseudo-capacitance for a fully covered surface is about 2000 μF. A high degree of accuracy is possible at low coverages. By this method it has been shown that in acid iron at its corrosion potential is covered to about 3-5%. The method needs evaluation over a range of cathodic potentials on iron in acid solutions.

6. Hydrogen Permeation Current Method

Small permeation rates of hydrogen through metals can be

measured directly and accurately by anodic dissolution. This eliminates the main disadvantage of the permeation method and enables the evaluation of θ in any solution, and is potentially the most useful method hitherto developed. The theory and preliminary results are discussed later in this report.

EXPERIMENTAL INVESTIGATIONS ON NICKEL

1. Determination of the degree of coverage of nickel in alkaline solution:

Nickel is susceptible to hydrogen embrittlement and is often used in strongly alkaline media. The double pulse galvanostatic method can be used with this system to determine the coverage and hence the mechanism. The coverage data thus obtained can be used in studies of embrittlement by metallurgical techniques in order to elucidate the relationship. For these reasons, this system was investigated.

2. Nickel Electrode

A B.D.H. nickel rod fitted with a polythene sleeve was used as the test electrode. A polythene rod 1/2 in. diam. and 2 in. long was drilled axially to an int. diam. of 3/32 in. A nickel rod 4 in. long and 1/8 in. diam. was then forced through the hole in the polythene rod to obtain a water-tight fit. The polythene-covered end was machined flat so as to expose only the area of cross-section (0.083 sq. cm.).

3. Cell and Auxiliary Electrodes

The cell (see fig. 1) was made of Pyrex glass and had three compartments. The diffusion of oxygenated anolyte into the test chamber was prevented by means of a sintered disc inserted between the compartments. The Luggin capillary from the reference electrode compartment was centered

vertically upwards in the test chamber. Provision was made to admit purified hydrogen into the test and reference electrode compartments through capillary tubes.

As anode, a bright sheet of platinum was used for the cathodic polarization of the test electrode. The reference electrode was an Ellis hydrogen electrode. In the test electrode compartment were the polythene-sleeved nickel electrode, and surrounding it, a platinum cylinder 3/4 in. diam. and 2 in. long. The platinum cylinder was used as the cathode, first during the pre-electrolysis and later, for the anodic polarization of the test electrode. These two electrodes were mounted on a polythene stopper, Figure 1. The central and reference electrode compartments had bubblers containing distilled water to prevent diffusion of air into the cell.

4. Electrolyte

Sodium hydroxide solution (2 N) was used as the electrolyte. Merck's pellets (extra pure quality) of sodium hydroxide were dissolved in conductivity water, which was prepared by previously reported methods. The specific conductivity of this water was 0.4 μmhos.

5. Purification of Hydrogen

Tank electrolytic hydrogen was deoxygenated by passage through a palladized asbestos furnace. The gas was bubbled through water and fed by polythene tubing to the test and reference electrode compartments. The rate of bubbling of hydrogen was controlled by plastic aquarium-type regulator valves.

6. Electrical Circuit

The circuit used is given in Figure 2. There were two polarizing

circuits - one to polarize the Ni electrode cathodically and the other to polarize it anodically. The Ni electrode was first polarized cathodically and the change-over to anodic polarization effected instantaneously. This was achieved by using a mercury-wetted relay with a rise time of 10^{-7} sec. The cathodic polarizing circuit was always on, and on switching on the anodic current by means of this relay, the test electrode became anodically polarized. Since the anodic current was at least a hundred times larger than the cathodic current, the effect of the latter is negligible when calculating the anodic c.d. Leakage of the anodic pulse into the cathodic polarizing circuit was minimized by a high-capacity choke.

For cathodic polarization, a battery-powered circuit was used, the current being measured by a Cambridge unipivot multirange microammeter. For very small currents, the potential across a standard 10 x1 megohm resistor was measured with a Doran valve potentiometer, and the current calculated.

For anodic polarization, the current source was a high-capacity 90 V battery. The current through the circuit was varied by adjusting the resistance box, and since the resistance between the platinum cylinder and the test electrode was negligibly small, the anodic current was controlled only by this resistance.

7. The Relay

A Western Electric relay using mercury-wetted contacts in high-pressure nitrogen (type 275B) was used. It was operated by a 90 V battery and a microswitch with a suitable filtering circuit (Figure 3).

8. Measuring and Recording Apparatus

(a) Potentiometer: Doran pH meter reading to ±0.0005 V;

(b) Oscilloscope: Tektronix type 535 with 53/54 D high-gain differential d.c. amplifier;

(c) Camera: Exakta Varex IIA fitted with Makro Kilar D 1:2.8/4 cm.

9. Procedure

The cell, cleaned first with dichromate and sulphuric acid mixture, was washed thoroughly with distilled water. It was rinsed several times with sodium hydroxide before introducing the solution. The exposed area of the nickel electrode was scraped with a clean, grease-free blade to give a bright surface. The solution was pre-electrolyzed at 25 mA for 3-4 h using the bright platinum sheet as anode and the platinum cylinder as cathode. During pre-electrolysis, as well as during measurements, a steady stream of hydrogen was bubbled through the test and the reference electrode compartments.

After pre-electrolysis, hydrogen overpotential measurements were made in the c.d. range 10^{-1} to 10^{-6}, the test electrode being fitted so as almost to touch the Luggin capillary. Galvanostatic anodic charging was then commenced. The test electrode was polarized cathodically at a desired c.d., and an anodic pulse of predetermined magnitude passed through the nickel electrode by operating the microswitch. The Ni electrode immediately became anodic and the change of potential from cathodic to that of oxygen evolution was displayed on the oscilloscope. The transient was photographed on a fast green-sensitive recording film, using the Exakta camera fitted with the close-up lens (exposure for about 3 sec at B). For any combination of cathodic and anodic c.d., 2 transients, the normal and

the compensation, were obtained. The normal curve was that obtained starting from the equilibrium overvoltage at any cathodic c.d. The compensation curve was obtained immediately after the normal curve. On releasing the microswitch, there was only cathodic polarization of Ni and the potential of the electrode gradually changed from anodic to cathodic. The compensation curve was obtained by switching on the anodic polarization circuit when the potential of the Ni electrode had fallen to +25 to 50 mV, as measured by the potentiometer. The compensation curve obtained starting at +25 mV was nearly identical with that obtained starting at +50 mV, showing the absence of adsorbed hydrogen on the surface in this range. This is also supported by the low values for the capacity (20μF), calculated from the compensation curve. The film was placed in an enlarger and the oscilloscope trace was drawn on cm graph-paper at a linear magnification of four times the oscilloscope screen size. The gradients of the curves were obtained at various points by graphical differentiation using a front-silvered mirror and set square. All measurements were made at room temperature (26-28°C).

RESULTS AND CALCULATION

1. Overpotential Results

Overpotential measurements on Ni cathodes in alkaline solutions are only for dilute solutions.[6] These results, obtained with hydrogen-saturated wire electrodes, show that overpotential decreases with increasing alkali concentration. Our results are for electrodes which had not been previously heated in a hydrogen atmosphere. The lower energy of activation for the discharge of H^+ ion; consequently, is anotner factor

reducing overpotential values. Our results are shown in Figure 4. The reproducibility was ±2 mV at low c.d.'s rising to ±10 mV at high c.d.'s.

2. Calculation of q_H

Figure 5 shows a typical pair of galvanostatic charging curves. $(i_H - i_{an}\theta)$ at any potential was calculated from the gradients of the normal and the compensation curves. A plot of $(i_H - i_{an}\theta)$ against t_N, where t_N is the time required to reach this potential on the normal curve, is shown in Figure 6. The area under the curve then gives the quantity of electricity (q_H) required to dissolve all the adsorbed atomic hydrogen originally present on the cathodically polarized surface.

3. Variation of q_H with Anodic c.d.

Results at a constant cathodic c.d. of 10^{-4} are given in Figure 7. It shows that q_H has a constant value of about 55μC cm^{-2} at anodic c.d.'s above 0.6 A cm^{-2}. This means that re-adsorption of hydrogen is negligible at anodic c.d.'s above 0.6 A cm^{-2}. The results were reproducible to ±5μC in the regions where re-adsorption was absent.

4. Variation of q_H with Cathodic c.d.

The anodic c.d. was kept constant a 1 A cm^{-2}, since at this value there is no re-adsorption of hydrogen. The results given in Table 1 show that q_H values at cathodic c.d.'s exceeding 10^{-3} are very large, evidently due to re-adsorption from hydrogen bubbles sticking to the electrode. This phenomenon was also observed on noble metals by Breiter, Knorr and Volkl,[7] and on Ag by Devanathan, Bockris and Mehl.[8]

5. Degree of Coverage

The roughness factor (r.f.) was calculated from the capacity of the electrode, which had an average value of 20μF. Since the capacity

of the Hg electrode under cathodic polarization has been shown by various workers to have a value of 16 μF, the roughness factor of the nickel electrode was 1.25. The charge required to dissolve the hydrogen adsorbed on 1 sq. cm of Ni, assuming a 1:1 H:Ni ration, is 326 μC; hence, the charge required to dissolve a monolayer of hydrogen from 1 sq. cm of apparent area is equal to 326 x 1.25 = 400 μC.

Values of θ calculated in this way are given in column 4 of Table 1.

DISCUSSION

1. Mechanism of the Hydrogen-Evolution Reaction

The data obtained permit the determination of the stages involved in the cathodic evolution of hydrogen. The first step in the evolution of hydrogen must be the discharge of a hydronium ion (path A), or a water molecule (path B), yielding adsorbed atomic hydrogen on the Ni surface:

$$(A) \qquad H_3O^+ + Ni + e = NiH + H_2O$$

$$(B) \qquad H_2O + Ni + e + NiH + OH^-$$

In strongly alkaline solutions (2 N) path A is unlikely since the concentration of hydrogen ions is negligibly small, and it appears that path B is the first step in the formation of adsorbed atomic hydrogen.

The removal of this adsorbed atomic hydrogen from the surface could proceed either by electrochemical desorption (path C), or by Tafel recombination (path D);

$$(C) \qquad NiH + H_3O^+ e = H_2 + H_2O + Ni$$

$$(D) \qquad NiH + NiH = H_2 + 2Ni$$

2. Rate-Determining Step

Since path A is unlikely, any one of the steps B, C or D could be

TABLE 1

Variation of q_H and θ with Cathodic c.d. Anodic c.d. = 1 A cm^{-2}

cathodic c.d. (A cm^{-2})	n(mV)	$q_H(\mu C)$	θ
1.00×10^{-6}	10	18	0.045
1.00×10^{-5}	30	26	0.065
1.80×10^{-5}	37	26	0.066
3.00×10^{-5}	52	29	0.072
5.65×10^{-5}	70	42	0.104
1.00×10^{-4}	90	49	0.122
1.80×10^{-4}	121	72	0.179
3.00×10^{-4}	140	100	0.250
5.65×10^{-4}	166	121	0.303
1.00×10^{-3}	186	155	0.386
3.00×10^{-3}	242	1050	2.62
1.00×10^{-2}	802	3040	7.60
1.00×10^{-1}	460	10,440	25.55

rate-determining. It has been shown that when discharge is the rate-determining step, the stoichiometric number[9] is 2. This number v can be determined using the equation

$$v = 2i_o \frac{F}{RT} \frac{(d\eta)}{(di_c)_{\eta \longrightarrow o}} \qquad (1)$$

or, from the point at which the overpotential deviates from the Tafel line due to the ionization of hydrogen.[9] v is then given by the equation

$$v = V/0.038 \qquad (2)$$

where V is the potential at which there is the break in the overpotential curve. v calculated by both methods was found to be 2. Therefore, the rate-determining step in the evolution of hydrogen on nickel in strongly alkaline solutions is slow discharge from a water molecule. If slow discharge is the rate-determining step, it is reasonable to expect small values for θ. Figure 8 shows where θ is plotted as a function of log c.d. and indicates low coverage up to a c.d. of 5×10^{-4}. Thereafter, the extremely rapid rise is due to re-adsorption from hydrogen bubbles sticking to the electrode surface.

3. Desorption Mechanism

The desorption of adsorbed hydrogen atoms can proceed by Tafel recombination or by an electrochemical mechanism. If the former is the desorption step, then

$$i_c = k_T \theta^2 \qquad (3)$$

Electrochemical desorption can be fast, or slow and rate-determining. For the latter case,

$$i_c = k_E \theta \qquad (4)$$

For fast electrochemical desorption, θ should be independent of the c.d.

A plot of log i against log θ would therefore give a gradient of zero for fast electrochemical desorption, 1 for slow electrochemical desorption and 2 for Tafel recombination. The results plotted in this way are shown in Figure 9. The gradient is two, thus proving that Tafel recombination is the desorption step. It should be noted that this result is not affected by the value of roughness factor assigned in the calculation of θ, for only the intercept will be affected.

The value, $10^{-2.2}$, of i_c at log $\theta = 0$ gives the rate constant, in amps, for the recombination step.

4. The Tafel Equation

In the Tafel equation, based on the formula

$$i = i_o \exp(-\alpha nF/RT) \qquad (5)$$

i_o is the rate of discharge of hydrogen ions on 1 sq. cm of the electrode surface when $\eta = 0$. It is apparent that this i_o, commonly called the exchange current, is only a partial current, since even at the reversible potential there is some coverage with atomic hydrogen. In order to get the rate constant for the discharge of hydrogen ions, it is necessary to correct for the coverage. Therefore, the Tafel equation is modified to read:

$$i_c = \vec{i}_o(1-\theta) \exp(-\alpha nF/RT) \qquad (6)$$

where θ is the coverage at the overpotential η. Here i_c is the current through 1 sq. cm. of apparent area, the fraction θ being blocked for the discharge of H^+ ions (excepting an electrochemical desorption process); $\vec{i}_o$ is the c.d. for the discharge on a hydrogen-free surface when $\eta = 0$.

On plotting against log $i_c/(1-\theta)$ (Figure 10), it will be seen that above 75 mV the graph is a straight line, giving $\vec{i}_o = 10^{-4}$ A cm^{-5}

and b = 88 mV.

The deviations from the Tafel line at low cathodic c.d.'s are due to the reverse reaction (i.e., ionization) becoming appreciable. If, therefore, a quantitative correction is applied for this ionization current, then all the points should fall on a straight line when η is plotted against log $i_c(\text{corr.})/(1-\theta)$.

The measured cathodic current is the difference between the discharge and the ionization currents, i.e.,

$$i = \vec{i} - \overleftarrow{i} \qquad (7)$$

$\overleftarrow{i}$ must depend on θ and the overpotential. It is given in terms of $\overleftarrow{i_o}$ by the equation

$$\overleftarrow{i} = \vec{i_o}\theta \exp\ (1-\alpha)nF/RT \qquad (8)$$

Hence, the complete equation for the cathodic current, from equations (6), (7) and (8), is

$$i_c = \vec{i_o}\ (1-\theta) \exp\ (-\alpha nF/RT) - \overleftarrow{i_o}\theta \exp\ (1-\alpha)nF/RT \qquad (9)$$

This may be contrasted with an equation by Breiter, Knorr and Volkl:[7]

$$i_c = i_o \left(\frac{(1-\theta)}{(1-\theta R)} \exp \frac{(-\alpha nF)}{(RT)} - \frac{\theta}{\theta_R} \exp \frac{(1-\alpha)nF}{RT} \right) \qquad (10)$$

where i_o is supposed to be the exchange c.d.

If one puts $\theta = \theta_R$ and $\eta = 0$ in the above equation, $i_c = 0$, which means that $\vec{i} - \overleftarrow{i} = i_o$. As pointed out earlier, i_o cannot be the true c.d. as it is only a partial current on 1 sq. cm of a partly covered surface. In contrast, equation (9) reduces to

$$0 = \vec{i_o}\ (1-\theta_R) - \theta_R \overleftarrow{i_o} \qquad (11)$$

$\overleftarrow{i_o}$ can be equal to $\vec{i_o}$ only if $\theta_R = 1/2$. However, if θ_R is known, it is possible to calculate $\overleftarrow{i_o}$ from $\vec{i_o}$ by using the above equation. θ_R was determined by extrapolating a graph of θ against η to $\eta = 0$. A

straight line was obtained for overpotential values less than 50 mV and θ_R was found to have a value of 0.04.

Therefore,

$$\overleftarrow{i_o} = \overrightarrow{i_o}(1-0.04)/0.04 = 240\,\mu\text{A cm}^{-2} \qquad (12)$$

The validity of eqn. (9) can be checked in the following manner, writing it in the form

$$\frac{i_c + \overleftarrow{i_o}\theta \exp (1-\alpha)nF/RT}{1-\theta} = \overrightarrow{i_o} \exp \left\{\frac{-\alpha nF}{RT}\right\} \qquad (13)$$

and plotting the log of the left-hand term against overpotential (Fig. 10). It will be seen that all the points lie on the same line with $\overrightarrow{i_o} = 10^{-5}$ and the slope b = 88 mV (see Table 2).

Column V shows that the ionization current is approximately 10 μA throughout the range covered. At a c.d. of 10^{-4} it forms 10% of the total current, thus confirming Bockris and Potter's observation[9] that departure of the Tafel line from linearity is due to the ionization current. The results and the graph confirm the validity of eqn. (9).

5. Desorption Mechanism at High c.d.'s

Up to a c.d. of 10^{-3} A cm^{-2}, desorption is by Tafel recombination. The double charging method cannot be applied to determine θ at higher c.d.'s owing to errors arising from re-adsorption of hydrogen. The Tafel recombination rate constant is $10^{-2.2}$ and is the maximum rate corresponding to full coverage. It is therefore not possible for the electrode reaction to proceed by the slow discharge - fast recombination path, but must change over above 10^{-3} amp. cm^{-2} to slow discharge - fast electrochemical desorption in which case the coverage will be independent of the current density. Preliminary investigations by the hydrogen permeation

TABLE 2

I	II	III	IV	V	VI	VII
n(mV)	θ	$\frac{(1-\alpha)nF}{RT}\eta$	e^{-x}	$\overleftarrow{i_o\theta e^{-x}}$	$\frac{\overleftarrow{i_c+i_o\theta e^{-x}}}{1-\theta}$	$\log\frac{\overleftarrow{i_c+i_o\theta e^{-x}}}{1-\theta}$
10	0.045	0.123	0.887	9.60	11.1	1.045
30	0.065	0.355	0.705	11.00	22.5	1.352
37	0.066	0.453	0.638	11.20	30.2	1.480
52	0.072	0.600	0.549	9.45	42.5	1.628
70	0.104	0.833	0.436	10.80	75.	1.875
90	0.122	1.09	0.336	9.82	125.	2.097
121	0.179	1.45	0.237	10.18	232	2.365
140	0.250	1.70	0.183	11.0	414.	2.617
166	0.303	2.03	0.131	9.5	824.	2.916
186	0.386	2.30	0.100	9.32	1630.	3.212

current method seems to indicate a limiting coverage of about 0.4, which would make the electrochemical rate constant to be 1.5 times the discharge rate constant, i.e., 1.5×10^{-5}.

6. Attempted measurement of coverage on iron in alkaline solutions

Since calculations indicated that iron in alkaline solution could be studied by the double charging method,[2] experimental investigations on the same lines as on nickel were carried out. It was soon apparent that the method could not be applied on iron due to the large currents arising from hydrogen diffusing into the interface and dissolving at all anodic potentials. The double pulse method depends on the absence of diffusion of hydrogen either from the solution phase or, as in this case, from the bulk of the metal. This was indicated by the large capacities of the order of 2000-800 μF, which were observed on iron electrodes.[10] These values cannot be accounted for on the basis of a large roughness factor, and are due to an electrochemical reaction; i.e., anodic dissolution of hydrogen.

HYDROGEN PERMEATION CURRENT METHOD

INTRODUCTION

The above-mentioned difficulty encountered with iron in the application of the double charging galvanostatic method suggested an alternative approach to the measurement of coverage. This consists in the electrochemical evaluation of the rate of permeation of hydrogen by anodic dissolution. Previous investigations of hydrogen permeation depended on the measurement of the quantity of hydrogen permeating through at various intervals of time. This was achieved by measurement of the increase in volume at constant pressure or of the increase in pressure at constant volume. The possibility of measuring continuously the rate of hydrogen permeation as a function of time presents an opportunity to obtain data on coverage and also on the rate constants for the transfer of hydrogen to the bulk from the surface, for the transfer from bulk to surface, the diffusion constant within the bulk and also the hydrogen concentrations in the metal.

THEORY

Diffusion Theory Relevant to the Method.

Consider unit area of a membrane of thickness L and diffusion constant for hydrogen D (see Figure 11). Let the concentration of hydrogen at x=0 and x = L be maintained at C_1 and C_2 respectively. In the steady state the through-put of hydrogen is given by

$$P = D \frac{dc}{cx} \qquad (14)$$

and hence

$$P = D \frac{(C_1 - C_2)}{L}$$

For the non-stationary state the general solution of the Fick's law equation[11]

$$\frac{dc}{dt} = D \frac{\partial^2 c}{\partial x^2} \tag{16}$$

for this problem is

$$C_{xt} = C_1 + (C_2 - C_1)\frac{x}{L} + \frac{2}{\pi}\sum_{n=1}^{n=\infty} \frac{(C_2 \cos n\pi - C_1)}{n} \sin \frac{n\pi x}{L} e^{-\frac{Dn^2\pi^2 t}{L^2}}$$

$$+ \frac{4C_o}{\pi}\sum_{m=0}^{m=\infty} \frac{1}{(2m+1)} \sin \frac{(2m+1)\pi x}{L} e^{-\frac{D(2m+1)^2\pi^2 t}{L^2}} \tag{17}$$

where C_{xt} is the concentration at any point x at time t, and C_o is the initial concentration of hydrogen in the membrane. On dropping the term in C_o for membranes initially free of hydrogen, differentiating with respect to x and multiplying by D, the equation obtained is

$$D\left(\frac{dc}{dx}\right)_t = \frac{D(C_2 - C_1)}{L} + \frac{2D}{L}\sum_{n=1}^{n=\infty} (C_2 \cos n\pi - C_1) \cos \frac{n\pi x}{L} e^{-\frac{Dn^2\pi^2 t}{L^2}} \tag{18}$$

For the plane x=0 (18) yields

$$P_{(x=o)t} = \frac{D(C_2 - C_1)}{L} + \frac{2D}{L}\sum_{n=1}^{n=\infty} (C_2 \cos n\pi - C_1) e^{-\frac{Dn^2\pi^2 t}{L^2}} \tag{19}$$

where $P_{(x=o)t}$ is the permeation rate at x=o at time t. In the steady state, $t \longrightarrow \infty$, the exponential term is zero and reduces to

$$P_{(x=o)t_\infty} = \frac{D(C_2 - C_1)}{L} \tag{20}$$

Similarly for the plane x=L (18) gives

$$P_{(x=L)t} = \frac{D(C_2 - C_1)}{L} + \frac{2D}{L} \sum_{n=1}^{n=\infty} (C_2 \cos n\pi - C_1) \cos n\pi e^{-\frac{Dn^2\pi^2 t}{L^2}} \qquad (21)$$

which for $t \longrightarrow \infty$ becomes

$$P_{(x=L)t_\infty} = \frac{D(C_2 - C_1)}{L} \qquad (22)$$

The diffusion constant, D, may be evaluated from permeation transients in the following ways:

(a) Time lag method

This is the method[12] used hitherto, when only the quantity of hydrogen permeating was measurable as a function of time, i.e. $\int_0^t P_{(x=o)t} dt$ which is denoted Q_t. For this purpose integration of (19) from o to t yields

$$Q_t = \frac{D(C_2 - C_1)t}{L} - \frac{2L}{\pi^2} \sum_{n=1}^{n=\infty} \frac{(C_2 \cos n\pi - C_1)}{n^2} \left(1 - e^{-\frac{Dn^2\pi^2 t}{L^2}}\right) \qquad (23)$$

as $t \longrightarrow \infty$ (23) reduces to

$$Q_t = \frac{D(C_2 - C_1)t}{L} - \frac{2L}{\pi^2} \sum_{n-1}^{n=\infty} \left(\frac{C_2 \cos n\pi}{n^2} - \frac{C_1}{n^2}\right) \qquad (24)$$

Summation of the second term yields the simple form

$$Q_t = \frac{D(C_2 - C_1)t}{L} - L\left(\frac{C_2}{6} + \frac{C_1}{3}\right) \tag{25}$$

Equation (25) may be rewritten as

$$Q_t = \frac{D}{L}(C_2 - C_1)t\left[1 - \frac{L^2}{6D}\frac{(C_2 + 2C_1)}{(C_2 - C_1)}\right] \tag{26}$$

Thus the intercept T_{lag} (time lag) on the time axis of a Q_t - t plot for large t is given by

$$T_{lag} = \frac{L^2}{6D}\left(\frac{C_2 + 2C_1}{C_2 - C_1}\right) \tag{27}$$

When $C_2 >> C_1$ this yields

$$T_{lag} = \frac{L^2}{6D} \tag{28}$$

thus permitting the calculation of D. Plots of equations (23) and (26) are shown in Figure (12).

(b) Rise time constant

When the permeation rate can be continuously recorded, the diffusion constant can be calculated as follows. From equations (19) and (20) the following is obtained.

$$\frac{P_t - P_\infty}{(P_\infty)_{x=o}} = \frac{2}{C_2 - C_1}\sum_{n=1}^{n=\infty}(C_2 \cos n\pi - C_1)\, e^{-\frac{Dn^2\pi^2 t}{L^2}} \tag{29}$$

For $C_2 >> C_1$ (29) reduces to

$$\left(\frac{P_t - P_\infty}{P_\infty}\right)_{x=o} = -2\sum_{n=1}^{n=\infty}(-1)^n\, e^{-\frac{Dn^2\pi^2 t}{L^2}} \tag{30}$$

On substituting $1/t_o$ for $\frac{D\pi^2}{L^2}$, and expanding (30) the series form(31) is obtained

$$\left(\frac{P_t - P_\infty}{P_\infty}\right)_{x=o} = -2\left[-e^{-\frac{t}{t_o}} + e^{-\frac{4t}{t_o}} - e^{-\frac{9t}{t_o}} - - - -\right] \qquad (31)$$

This may be written as:

$$\left(\frac{P_t - P_\infty}{P_\infty}\right)_{x=o} = 2\left[1 - e^{-\frac{3t}{t_o}} + e^{-\frac{8t}{t_o}} - - - -\right] e^{-\frac{t}{t_o}} \qquad (32)$$

The term within the brackets is indeterminate when t=o for it could be unity or zero, depending on whether an odd n or even n is considered. On taking logarithms,

$$\log_e \left(\frac{P_t - P_\infty}{P_\infty}\right)_{x=o} = \log_e \left[1 - e^{-\frac{3t}{t_o}} + e^{-\frac{8t}{t_o}} - - - -\right] + \log_e 2 - \frac{t}{t_o} \qquad (33)$$

The log of the term within the brackets, though indeterminate at t=o, rapidly becomes zero as t increases. Hence a plot of $\log_e \left(\frac{P_t - P_\infty}{P_\infty}\right)_{x=o}$ versus t yields as gradient $1/t_o$ and intercept $\log_e 2$. Thus from the gradient of this graph D can be calculated, using the formula

$$\text{gradient} = \frac{1}{t_o} = \frac{D\pi^2}{L^2} \qquad (34)$$

(c) Time lag from rise transient.

The time lag T_{lag} given by equation (28) represents the time at which the diffusion process, if it could proceed always at steady state value, should start in order that the amount permeating will be the

same as that for the ordinary diffusion process in the steady state. An inspection of Figure (13) shows that this time is that which makes the area of the rectangle equal to that of the rise curve. That is, the vertically hatched area should be equal to the horizontally hatched region. It is easy to show that for an exponential curve of time constant t_o this point corresponds to a permeation rate of .6299 times the steady state value. Thus the interval from zero time to the time the permeation rate is .6299 times the steady state value is L. Hence

$$T_{lag} = \frac{L^2}{6D} = t_{.6299} \tag{35}$$

(d) Time of initial rise

For an exponential curve the time taken to obtain .6299 time the steady state value is the its time constant. Hence, if t_i represents the time at which the permeation rate begins to rise from zero, the connection between these quantities as shown by Figure (13) is

$$T_{lag} = t_i + t_o \tag{36}$$

Therefore from t_i the diffusion constant can also be obtained with the formula

$$t_i = \frac{L^2}{D}\left(\frac{1}{6} - \frac{1}{\pi^2}\right) = \frac{L^2}{D\ 15.3} \tag{37}$$

(e) Decay time constant

Equation (17) is the general solution when an initially uniform concentration exists in the membrane. If the concentration were some function of x in the membrane, the general solution is given by

$$C = C_1 + (C_2 - C_1)\frac{x}{L} + \frac{2}{\pi}\sum_{n=1}^{n=\infty} \frac{(C_2 \cos n\pi - C_1)}{n} \sin\frac{n\pi x}{L}\, e^{-\frac{Dn^2\pi^2 t}{L^2}}$$

$$+ \frac{2}{L}\sum_{n=1}^{n=\infty} \sin\frac{n\pi x}{L}\, e^{-\frac{Dn^2\pi^2 t}{L^2}} \int_0^L f(x') \sin\frac{n\pi x'}{L}\, dx' \qquad (38)$$

Where $C = C_1$ at $x=o$ for all t

$C = C_2$ at $x=L$ for all t

$C = f(x)$ at $t=o$ for $0 < x < L$

If the steady state has been established in a membrane initially free of hydrogen, then the concentration gradient is uniform and is C_1 at $x=o$ and C_2 at $x=L$. If now the source of hydrogen is suddenly stopped and the time reckoned from this point, it follows that the initial distribution function required in the second term of equation (38) is simply

$$f(x') = \frac{(C_2 - C_1)x}{L} \simeq \frac{C'x}{L} \qquad (39)$$

The decay of the permeation at $x=o$ may then be described by equation (38) with the boundary conditions

$C = C_1 \simeq 0$ at $x=o$ for all t

$C = C_2 = 0$ at $x=L$ for all t

$C = f(x) = \frac{C'x'}{L}$ at $t=o$ for $0 < x' < L$

Under these conditions, (38) reduces to

$$C = \frac{2}{L}\sum_{n-1}^{n=\infty} \sin\frac{n\pi x}{L}\; e^{-\frac{Dn^2\pi^2 t}{L^2}} \int_0^L a(x') \sin\frac{n\pi x'}{L}\, dx' \qquad (40)$$

where $a = \frac{c'}{L}$ (41)

Integration by parts of (40) yields

$$C = \frac{2}{L}\sum_{n=1}^{n=\infty} \sin\frac{n\pi x}{L}\; e^{-\frac{Dn^2\pi^2 t}{L^2}} x\left\{\left[-\frac{ax'L}{n\pi}\cos\frac{n\pi x'}{L}\right]_0^L + \int_0^L \cos\frac{n\pi x'}{L}\right\} \qquad (42)$$

The last term is zero and substitution for the limits (42) becomes

$$C = \frac{2}{L}\sum_{n=1}^{n=\infty} \sin\frac{n\pi x}{L}\; e^{-\frac{Dn^2\pi^2 t}{L}} \left(-\frac{aL^2}{n\pi}(-1)^n\right) \qquad (43)$$

Or

$$C = \frac{2aL}{\pi}\sum_{n=1}^{n=\infty} \sin\frac{n\pi x}{L}\; e^{-\frac{Dn^2\pi^2 t}{L}} \frac{(-1)^{n+1}}{n} \qquad (44)$$

Differentiating with respect to x

$$\left(\frac{dc}{dx}\right)_t = 2a\sum_{n=1}^{n=\infty} \cos\frac{n\pi x}{L}\; e^{-\frac{Dn^2\pi^2 t}{L^2}} (-1)^{n+1} \qquad (45)$$

Multiplying by D and substituting x=o (45) becomes

$$P_{x=o,t} = 2aD \sum_{n=1}^{n=\infty} (-1)^{n+1} e^{-\frac{Dn^2\pi^2 t}{L^2}} \qquad (46)$$

Using the symbol t_o for $\frac{L^2}{D\pi^2}$ as before and expanding (46) may be written as

$$P_{x=o,t} = 2aD\, e^{-t/t_o} (1 - e^{-3t/t_o} + e^{-8t/t_o} - - - -) \qquad (47)$$

For t=o, let the permeation be $P_{(x=o)t=o}$. For reasons already given (p. 22) only the first term of the series is important and hence (47) can be transformed into

$$P_{x=o,t} = P_{(x=o)} e^{-t/t_o} \qquad (48)$$

Hence a plot of log, $(\frac{Pt}{Po})_{x=o}$ against time has a gradient $\frac{1}{t_o}$ and thus the diffusion constant can be calculated with the aid of the formula

$$\text{Gradient} = \frac{1}{t_o} = \frac{D\pi^2}{L^2} \qquad (49)$$

The above analysis shows that the diffusion constant may be evaluated by five different methods when transients can be recorded.

Formulae for the Determination of Coverage

Consider the same membrane but let some electrochemical reaction produce a steady state coverage with adsorbed atomic hydrogen θ_H at the interface at x=L. Let the opposite interface at x=o be maintained at some anodic potential sufficient to cause repidly any hydrogen atoms on the surface, thereby producing a steady coverage of zero. Let

the rate constant for the transfer of hydrogen from the surface into the metal be $k^{s \to b}$ and for the reverse process, $k^{b \to s}$. In the absence of any diffusion process within the membrane, let the equilibrium concentration of hydrogen in the metal at x=L be C_e. This equilibrium is represented by the equation

$$k^{s \to b} \theta_H = k^{b \to s} C_e \tag{50}$$

If due to a diffusion process within the membrane the concentration at x=o is altered from C_e to C_2, then the permeation of hydrogen into the membrane is given by

$$(k^{b \to s} C_e - k^{b \to s} C_2) = P \tag{51}$$

For steady state diffusion within the membrane, the concentration gradient is uniform, and if the concentration in the membrane at x=o is C_1 the rate of permeation is given by

$$\frac{D(C_2 - C_1)}{L} = P \tag{52}$$

At the interface at x=o the equilibrium is

$$k^{b \to s} C_1 = P \tag{53}$$

From (50), (51), (52) and (53) the following equation is obtained:

$$\frac{1}{P} = \frac{1}{D\Theta}\frac{\overset{b\rightarrow s}{k}}{\underset{k}{s\rightarrow b}} + \frac{2}{\underset{k}{s\rightarrow b}_{\Theta}} \tag{54}$$

The gradient of a plot of $\frac{1}{P}$ against L is given by

$$g = \frac{\overset{b\rightarrow s}{k}}{\underset{k}{s\rightarrow b}_{D\Theta}} \tag{55}$$

and its intercept by

$$I = \frac{2}{\underset{k}{s\rightarrow b}_{\Theta}} \tag{56}$$

The minimum values of g and I are reached with $\Theta \longrightarrow 1$, hence

$$g_m = \frac{\overset{b\rightarrow s}{k}}{\underset{k}{s\rightarrow b}_{D}} \tag{57}$$

and

$$I_m = \frac{2}{\underset{k}{s\rightarrow b}} \tag{58}$$

Hence Θ can be calculated using the equation

$$\Theta = \frac{g_m}{g} = \frac{I_m}{I} \tag{59}$$

In the above deduction it has been assumed that diffusion is the rate controlling process, i.e., $\underset{k}{s\rightarrow b}$, $\overset{b\rightarrow s}{k} >> D$. Under these conditions, the formulae previously deduced for the evaluation of D apply, and hence

D can be obtained independently. Therefore, with the aid of (57) and (58) both rate constants can be evaluated with a knowledge of D obtained from an analysis of the transients. When diffusion is rate controlling, the permeation rate will depend on the thickness of the membrane used according to equation (15). When $k^{s \rightarrow b}$ and $k^{b \rightarrow s}$ are both smaller than D, then, the surface reaction is rate controlling. In this case the permeation rate will be independent of the thickness of the membrane.

EXPERIMENTAL

Preliminary investigations to ascertain the scope and applicability of the proposed hydrogen permeation current were carried out as follows:

Cell:

This consisted of two symmetrical units each consisting of a 3/4" pyrex pipe flange to which was fused a large test tube with a 24/45 ground joint. It was fitted with a hydrogen reference electrode with a long tapering Luggin capillary terminating at the pipe flange as shown in Fig. 14a. Arrangements were made as illustrated to admit hydrogen or nitrogen gas to all four compartments each of which carried a platinised platinum electrode and a bubbler fused to its cap. The edges of the flanges were polished flat and by bolting together the two units on the test membrane with a teflon washer a liquid tight seal was made.

Hydrogen:

Tank hydrogen was deoxygenated by bubbling through ammonium vanadate solutions reduced with zinc amalgam. The gas was scrubbed with acid and water in wash bottles before admission to the cell.

Nitrogen:

"Prepurified" grade of nitrogen from cylinders was used.

Electrolyte Solutions:

These were prepared with conductivity water and analytical reagent grade chemicals. Alkaline solutions were 0.1N NaOH and acid solutions 0.1N sulphuric acid prepared as above.

Pilet's Bath:

$PdCl_2\ 2H_2O$	3.8 g	Made to one litre
$Na_2\ HPO_4$	100 g	Plating current density
$(NH_4)_2\ HPO_4\ 12H_2O$	20 g	3ma at 60°C.
Benzoic acid	2.4 g	

Electrical Circuits:

(a) Cathode Polarising Circuit: The power source was a 30v transistor supply unit. A variable current was obtained with the aid of two potentiometers each of 5K connected as shown in Fig. 14b. The current was measured with a Simpson multirange microammeter.

(b) Anodic Circuit: The out-put from the polarising bridge of a Sargent Model XV polarograph was applied to the membrane and its auxiliary electrode. The recorder was used to register the current at the required sensitivity setting.

Membrane Materials:

Shim steel, Nickel, Palladium and palladium plated steel were used. The surface was degreased with ether and alcohol before assembly in the cell. Palladium coatings were deposited electrolytically in a Pilet's bath at a temperature of 60°C.

Procedure:

The cell was cleaned in nitric sulphuric acid mixture washed thoroughly with distilled water and rinsed with conductivity water. The membrane carefully degreased was then bolted into position. The electrolytes were admitted to each unit and hydrogen allowed to bubble through. In the anodic polarising section, nitrogen was used for experiments with palladium and palladated steel, the electrolyte being

always 0.1N sodium hydroxide. A predetermined anodic potential was then applied and the recorder switched on. The current soon dropped to a very small steady value, the residual current. The cathodic circuit previously set to give a constant cathodic current of a desired magnitude, was then switched on and a mark made on the chart at this instant. After a short period the diffusing hydrogen produced an increasing current in the anodic circuit which was seen to read a steady state. After steady state was established the cathodic current was switched off and the decay transient also recorded. Such measurements were made with various electrolytes, cathodic current densities and anodic potentials. All measurements were at room temperature.

RESULTS

Exploratory measurements with steel, nickel and palladium showed that the method was sufficiently sensitive in the current density range 10^{-6} to 10^{-3}. Qualitatively the transients showed the gradation in diffusion constants which were expected, and also the variation with cathodic current density. With steel in acid and alkaline solutions at the same cathodic current density, the hydrogen hydrogen current was found to be larger by about a factor of 10 in accordance with the expected higher coverage with hydrogen in acid solution as compared to alkaline solutions.

The diffusion equations derived were then tested with Palladium in alkaline solutions. The rising and decay transients were recorded. These followed the pattern shown in Fig. 13 and are therefore not illustrated separately. The diffusion constant was calculated by

methods (a) - (e) using equations (28)(34)(35)(37) and (49). The linear plots predicted by equations (33) and (48) were obtained and the intercept of log 2 required by (33) was also verified, see Fig. 15 and 16. The diffusion constants calculated from the transients by the different formulae are given in Table 3.**

The diffusion constant when thus determined for steel in acid solutions was found to be 9.2×10^{-8}. The hydrogen permeation current was found to be constant in the anodic potential range 600 to 950 hence for these measurements the applied potential was always 750 mv. In order to eliminate the possibility of the formation of passive films which may alter the diffusion process, experiments were carried out with palladium plated membranes. The plating was deposited electrolytically in a Pilet's bath at 60°C. The thickness of the deposit was calculated by weighing the membrane before and after plating for a fixed period of time. Thereafter the desired thickness was obtained by reducing the period of plating proportionately at the same current density. Calculations showed that with deposits of Palladium of thickness .001 to .005 cm on a steel sheet of thickness .014 cm the diffusion constant should not be altered. Determination of the diffusion constant for plated membranes by the above mentioned formulae gave the identical result, but the permeation current was about two

---

** For the decay transient in Fig. (16) the mean straight line has been drawn. The diffusion constant thus obtained was found to be within 3% of the rise transient diffusion constant. However the points seem to suggest two slopes, the initial slope being identical with the rise slope but at larger times the slope is less suggesting a smaller diffusion constant when the mean hydrogen concentration is low. This is evidence for the first time of the variation of diffusion constant with concentration in solid metals. Previous observers could not have detected this effect as their technique was not sufficiently sensitive.

orders of magnitude larger. The reasons for this behaviour are discussed later. Table 4 gives the diffusion constants measured for various materials.

The permeation current in steel of thickness .0051 cm as a function of cathodic current density in acid and alkaline solutions is shown graphically in Figs. 17 and 18. These results are with unpalladated membranes at a constant anodic potential of 750 mV.

Discussion:

The consistency in the diffusion constant and the reproducibility of the results on palladium are worthy of note. As is well known despite the variety of methods used to measure the diffusion constants in palladium, no concordant values are reported in the literature.[13] Hence a comparison with the result obtained by the present method is not possible. In the first place most data on diffusion constants were obtained at elevated temperatures where the mechanism of diffusion is probably different from that here. A comparison with values obtained by extrapolation of this data is not therefore justified. It is also well known that the phase of a solid metal determines the diffusion constant. In the literature data, the diffusion constant was obtained in many cases by following the increase in volume of hydrogen at constant pressure. This procedure would mean that the palladium used was β-palladium. In the method used hydrogen is removed by anodic polarisation and the mean hydrogen concentration would be small and the diffusion constant would therefore be that for α-palladium.

With steel sheet the diffusion constant obtained is smaller than that for palladium, that for nickel was intermediate. As expected the diffusion constant measured was not changed when the steel membrane was palladated with a layer .001 - .0005 cm thick. But the increased current needs explanation. Although in alkaline solutions susceptibility to passivation is great at anodic potentials, and such passivating layer will be reduced by the diffusing hydrogen. In the absence of passivating layer the explanation of this observation can be found on the Tafel recombination reaction at this surface. When hydrogen atoms diffuse into the surface, they can undergo the following reaction:

$$H + H \longrightarrow H_2 \qquad \text{Tafel recombination}$$

$$H \longrightarrow H^+ + e \qquad \text{Anodic dissolution}$$

The Tafel recombination reaction thus competes with the anodic dissolution reaction, and hence the magnitude of the observed dissolution current will depend on the relative values of their rate constants. The Tafel rate constant has been found to be $10^{-2.2}$ on nickel[14] in alkaline solutions and a similar value may be expected for iron in alkaline solution. Thus even at the high anodic potential recombination could appreciably decrease the hydrogen available for ionisation. In the absence of information on the i_o values for the hydrogen evolution reaction on iron in alkaline solution a calculation of relative magnitudes is not possible. When a thin layer of palladium is deposited, the situation changes for the recombination step is known to be slow and rate determining on palladium. Hence all the hydrogen will be removed by ionisation only and the observed current will therefore be larger. Since the palladium layer does not alter the diffusion

processes the use of palladated membranes as a standard procedure serves to enhance the sensitivity of the method. Previous investigators were unable to work at current densities below 10^{-3} amp as the amount evolved was beyond the sensitivity of their method of detection. This is also unfortunate as it is well known at above 10^{-3} amp/cm^2 blister formation[15] occurs on iron and may radically alter the nature of the cathodic surface. This has been confirmed in this work and it has been found that whereas below 10^{-3} the permeation current is a function of cathode current density, above 10^{-3} amp a hysteresis effect is observed and the diffusion constant and permeation are found to change beyond this point. This indicates that the surface structure undergoes some irreversible alteration.

With acid solutions, it is seen from Fig. 17, that the limiting current is 32μA. If this is assumed to correspond to full coverage, the coverage in alkaline solution is about 30% at the highest c.d. used. The gradient of the log 1_H vs log 1_c is about .5 and suggests that the square of the coverage is proportional to the cathodic current density which would be relationship of the hydrogen evolution reaction in slow discharge followed by fast Tafel recombination. Values for various current densities may be calculated from the data used for the graphs in Figs. 17 and 18. The accurate calculation of θ and of $s \underset{k}{\rightarrow} b$ and $b \underset{k}{\rightarrow} s$ requires data with membranes of known composition and varying thickness. Experiments to provide this data are in progress with the anodic potentials controlled with the aid of an electronic potentiostat.

TABLE 3

	Equation	Method	Quantity measured	D_{cm} sec^{-1}
1	(28)	Time lag by integration	L = 560 sec.	5.84×10^{-8}
2	(35)	Time lag from $t_{.63}$	L = 567 secs.	5.77×10^{-8}
3	(36)	Time of initial rise	t_1 = 213 secs.	6.02×10^{-8}
4	(34)	Gradient of log plot of rise curve	t_o = 335 secs.	5.94×10^{-8}
5	(35)	Gradient of log plot of decay curve	t_o = 342 secs initial	5.81×10^{-8}
			(t_o = 352 secs mean)	5.64×10^{-8}
			(t_o = 363 secs final)	5.47×10^{-8}
			Mean value (1 - 5)	$5.88 \pm .08 \times 10^{-8}$

TABLE 4

Material	Diffusion Constant
Palladium	5.88×10^{-8}
Steel	9.2×10^{-9}
Steel Palladated	9.3×10^{-9}
Nickel	$1\text{-}10 \times 10^{-8}$

ACKNOWLEDGEMENTS

Thanks are due to the following for their assistance in this project.

Mr. S. Srinivasan, for discussions on the mathematics of diffusion.

Mr. M. Selvaratnam, for investigations on nickel.

Mr. Z. Stachurski, for investigations of permeation rates.

REFERENCES

1. Bockris and Devanathan, ONR Technical Report No. 1. ONR 551(22).
2. Bockris and Colum, ONR Technical Report No. 2. ONR 551(22)
3. Bockris and Thacker, ONR Technical Report No. 3. ONR 551(22)
4. Conway, Proc. Roy. Soc., A247, 400 (1958).
   Kodera and Saito, J. Res. Inst. Catalysis, 1, 5 (1959).
5. Bockris and Kita, In press.
6. Bockris and Potter, J. Chem. Physics 20, 614 (1952).
7. Breiter, Knorr and Volkl, Z. Elektrochem., 59, 681 (1955).
8. Devanathan, Bockris and Mehl, J. Electroanalytical Chem., 1, 143 (1959/60).
9. Bockris and Potter, J. Electrochem Soc. 99, 169 (1952).
10. Devanathan and Srinivasan, unpublished.
11. Barrer, Diffusion in and through Solids, Cambridge (1941).
    Jost, Diffusion, Academic Press (1960).
    Crank, Mathematics of Diffusion, Oxford (1957).
    Barrer, Phil. Mag., 28, 148 (1939).
12. Daynes, Proc. Roy. Soc., A97, 286 (1920).
    Barrer, Trans. Faraday Soc., 35, 628 (1939).

13. Barrer, Diffusion in and Through Solids, Cambridge (1941) p. 219.

14. Devanathan and Selvaratnam, Trans. Faraday Soc., 56, 1820 (1960).

15. Thompson and Ubbelohde, J. Appl. Chem. 3, 27 (1953).

Raczymska and Smialowski, Bulletin de Academie Polonaise de Sciences 8, 209 (1960).

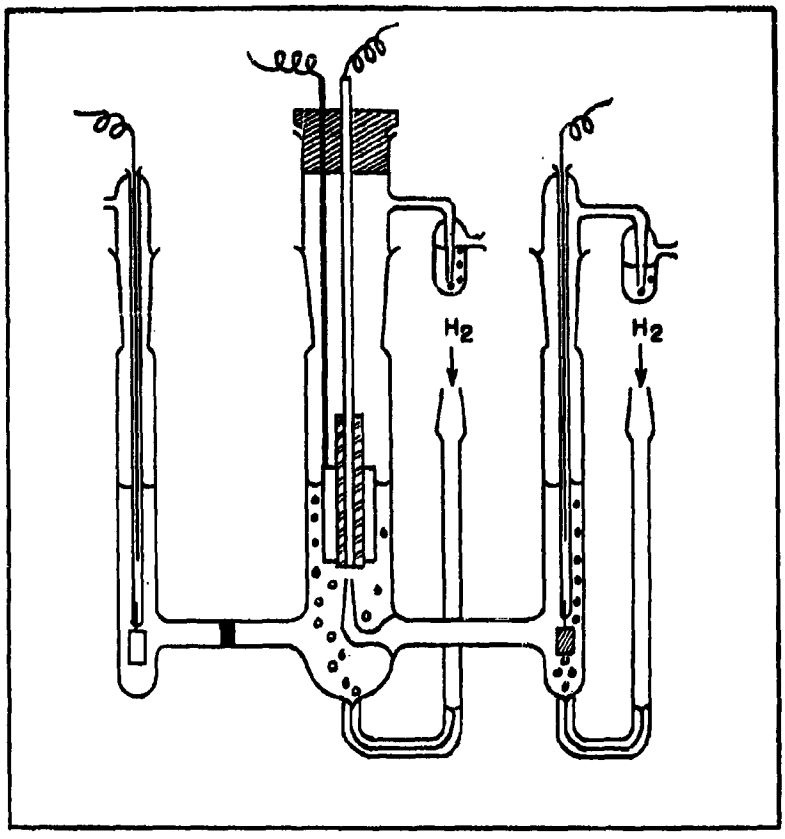
H2
H2

FIG. 1

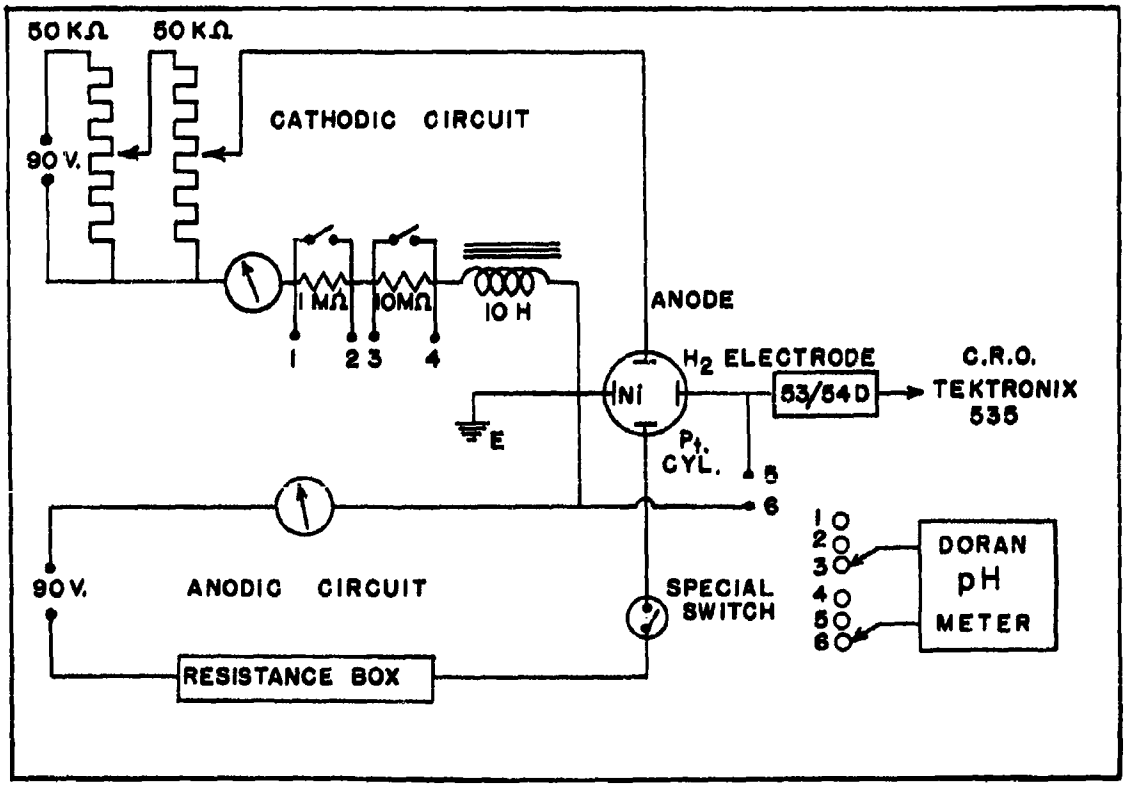
50 KΩ
50 KΩ
CATHODIC CIRCUIT
90 V.
1 MΩ
10MΩ
10 H
1
2
3
4
ANODE
H2 ELECTRODE
Ni
53/54D
C.R.O.
TEKTRONIX
535
E
Pt.
CYL.
5
6
1
2
3
4
5
6
DORAN
pH
METER
90 V.
ANODIC CIRCUIT
SPECIAL
SWITCH
RESISTANCE BOX

FIG. 2

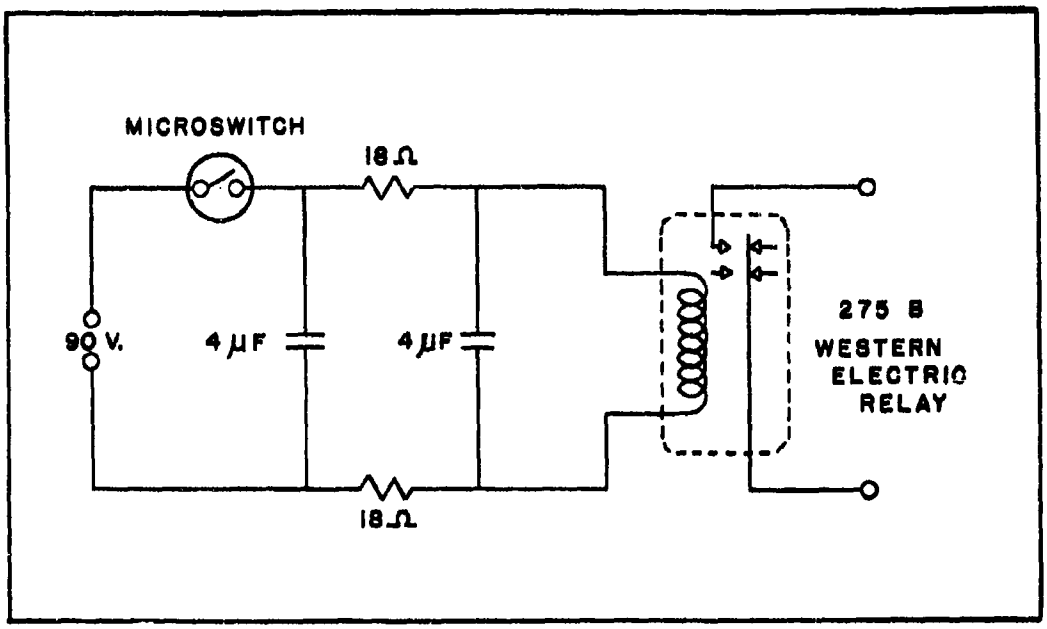
MICROSWITCH
18 Ω
90 V.
4 μF
4 μF
18 Ω
275 B
WESTERN
ELECTRIC
RELAY

FIG. 3

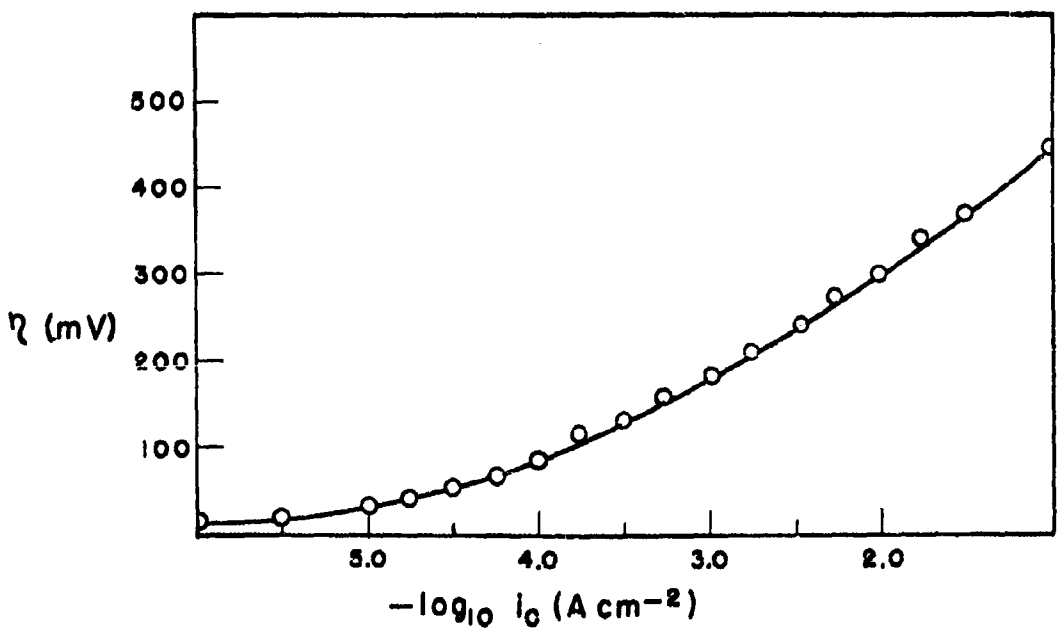
η (mV)
500
400
300
200
100
5.0
4.0
3.0
2.0
$-\log_{10} i_0$ (A cm^{-2})

FIG. 4

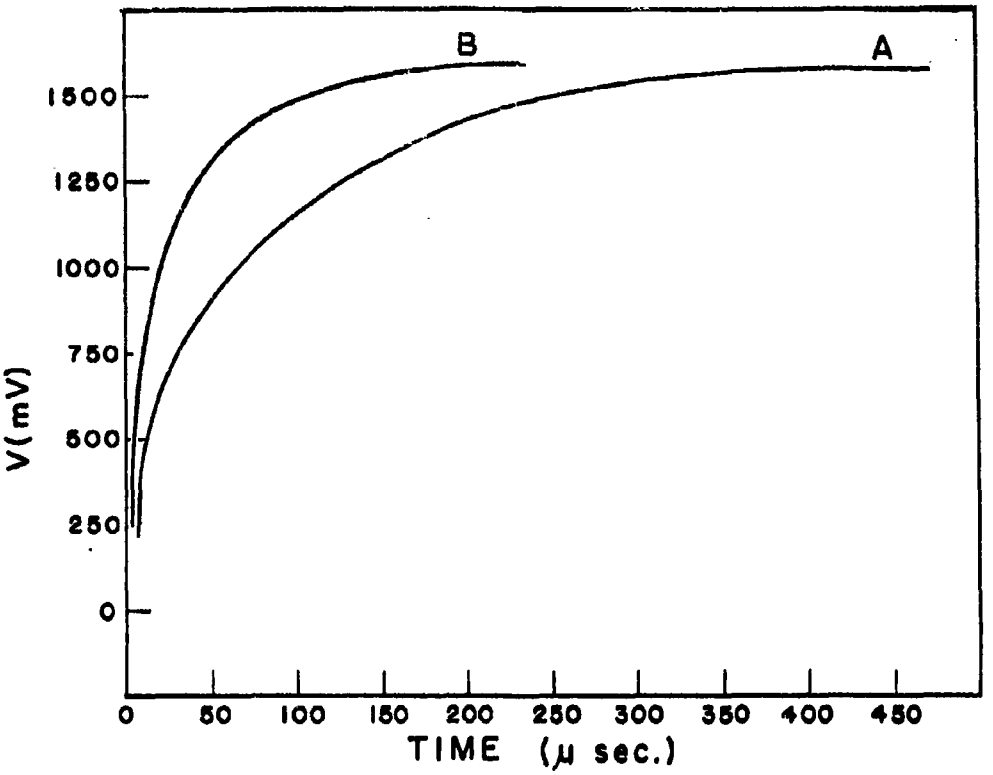
B
A
1500
1250
1000
750
500
250
0
V(mV)
0
50
100
150
200
250
300
350
400
450
TIME (μ sec.)

FIG. 5

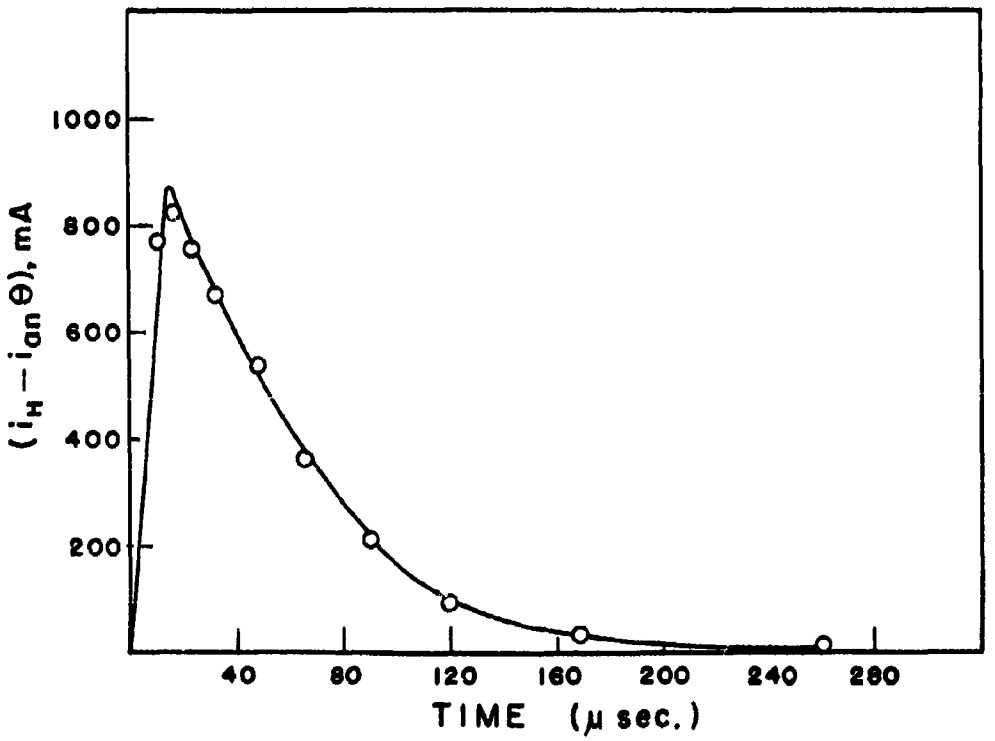
1000
800
600
400
200
$(i_H - i_{an}\theta)$, mA
40
80
120
160
200
240
280
TIME (μ sec.)

FIG. 6

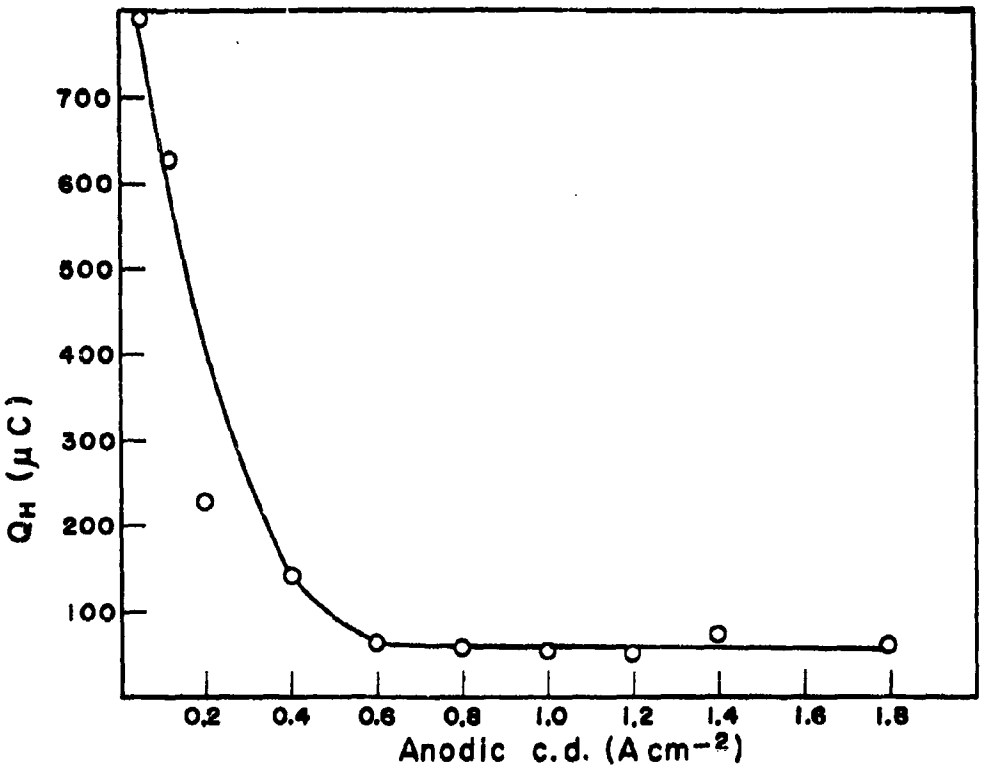
700
600
500
400
300
200
100
Q_H (μC)
0.2
0.4
0.6
0.8
1.0
1.2
1.4
1.6
1.8
Anodic c.d. (A cm^{-2})

FIG. 7

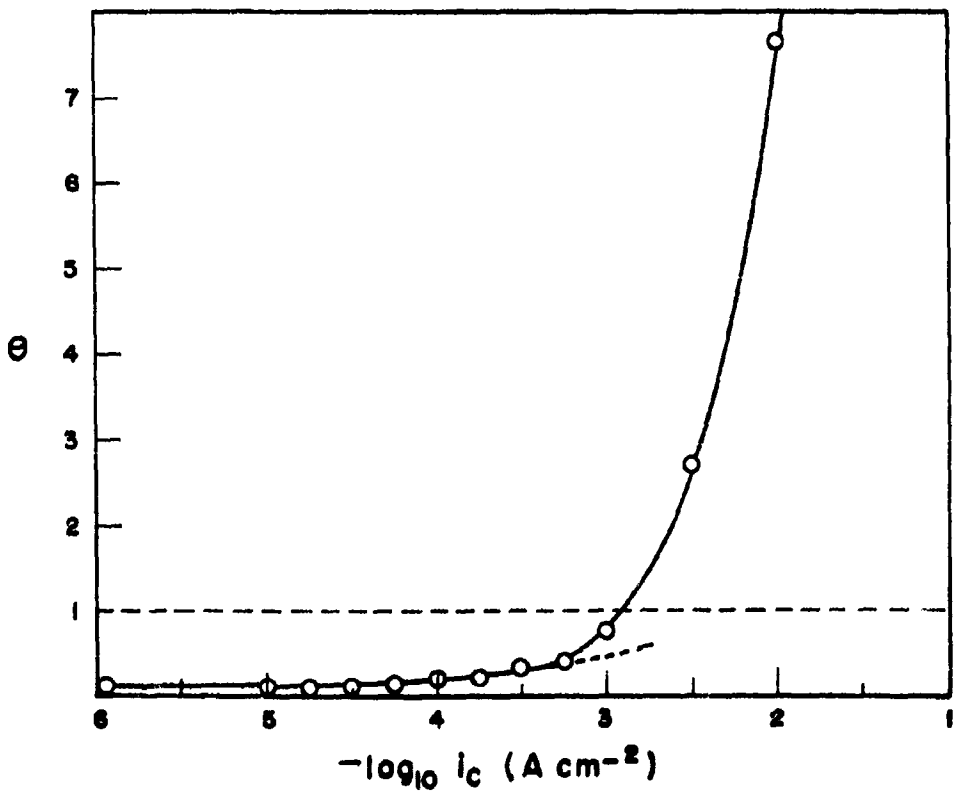
7
6
5
4
3
2
1
θ
6
5
4
3
2
1
$-\log_{10} i_c$ (A cm^{-2})

FIG. 8

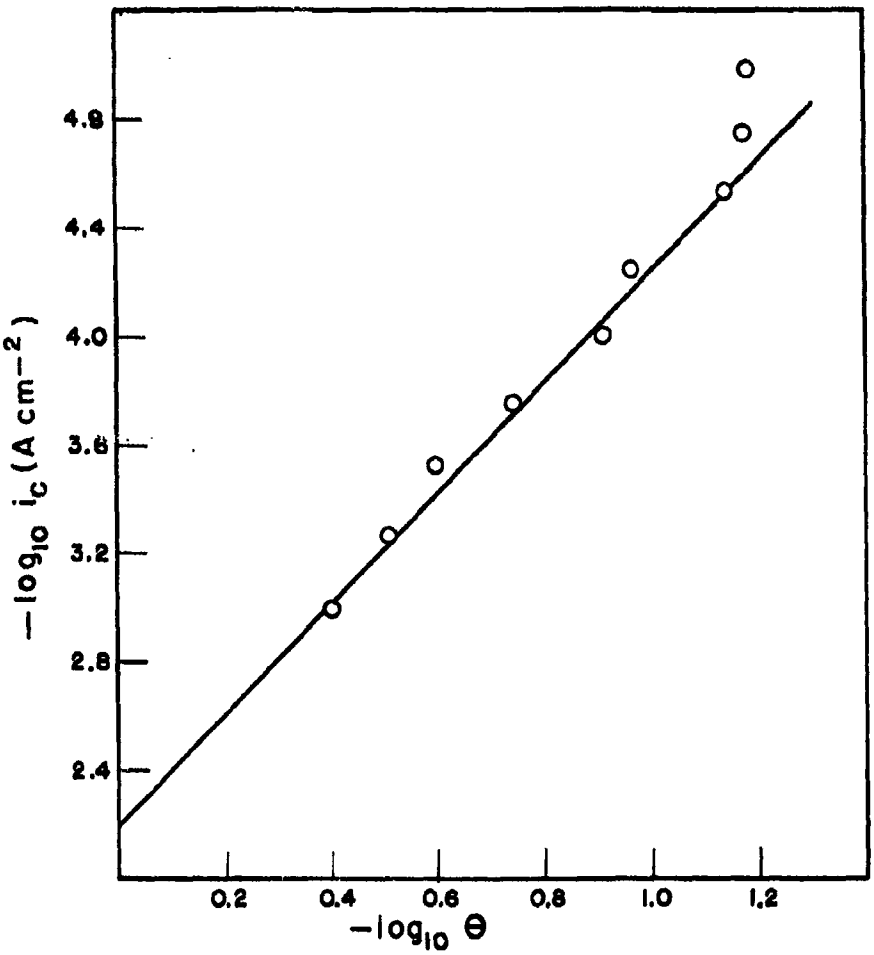
4.8
4.4
4.0
3.6
3.2
2.8
2.4
$-\log_{10} i_c$ (A cm^{-2})
0.2
0.4
0.6
0.8
1.0
1.2
$-\log_{10} \theta$

FIG. 9

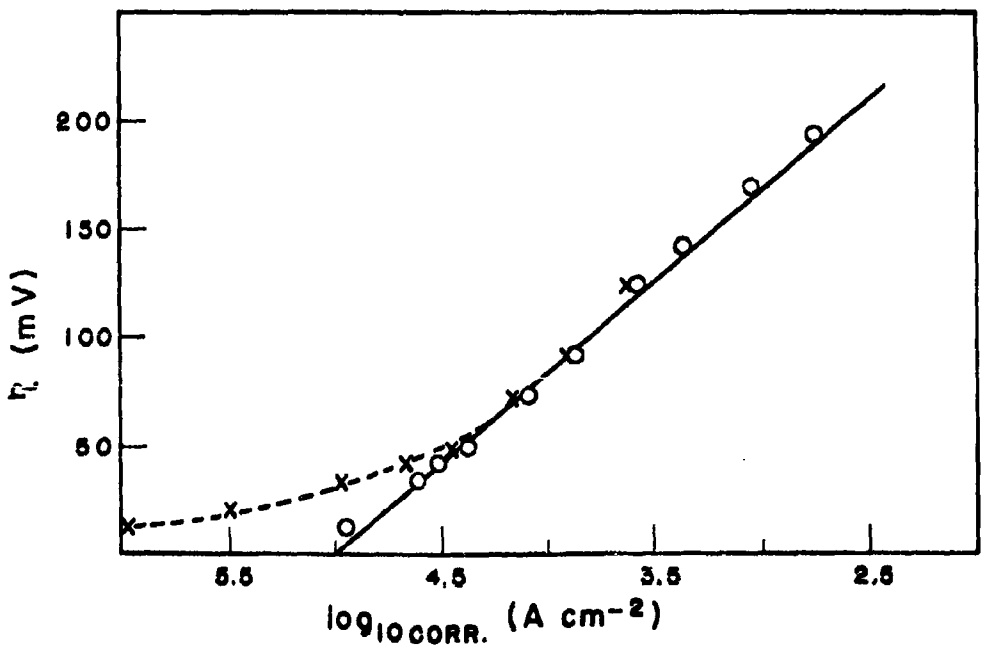
200
150
100
50
E (mV)
5.5
4.5
3.5
2.5
$\log_{10 CORR.}$ (A cm^{-2})

FIG. 10

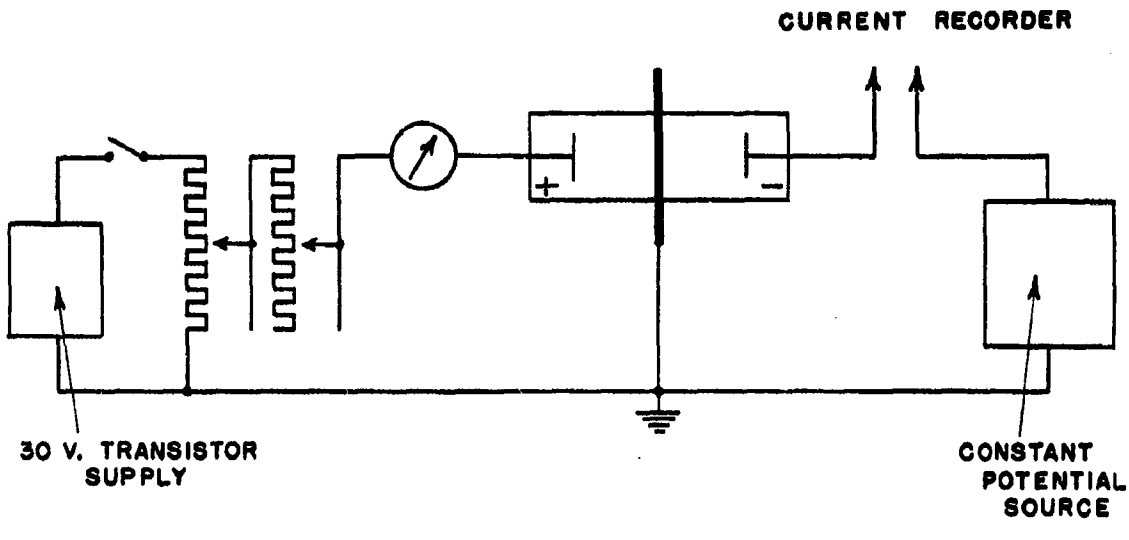

FIG. 14b

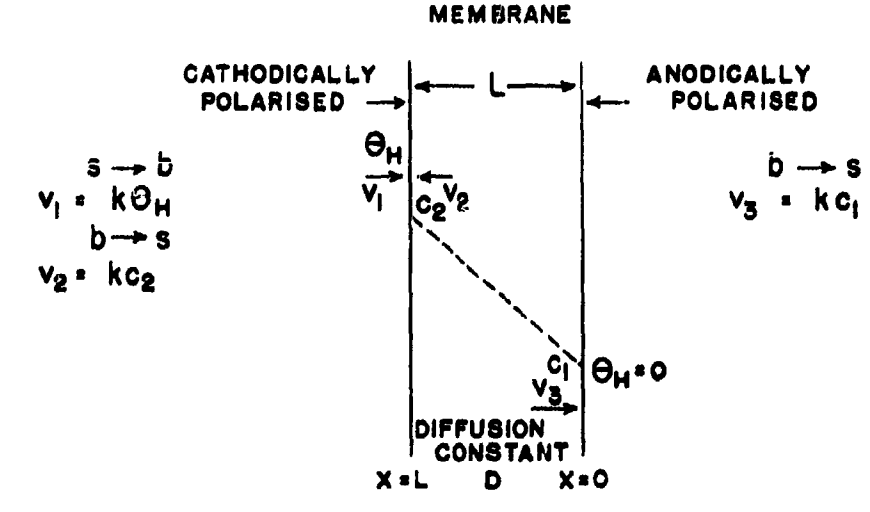

FIG. 11

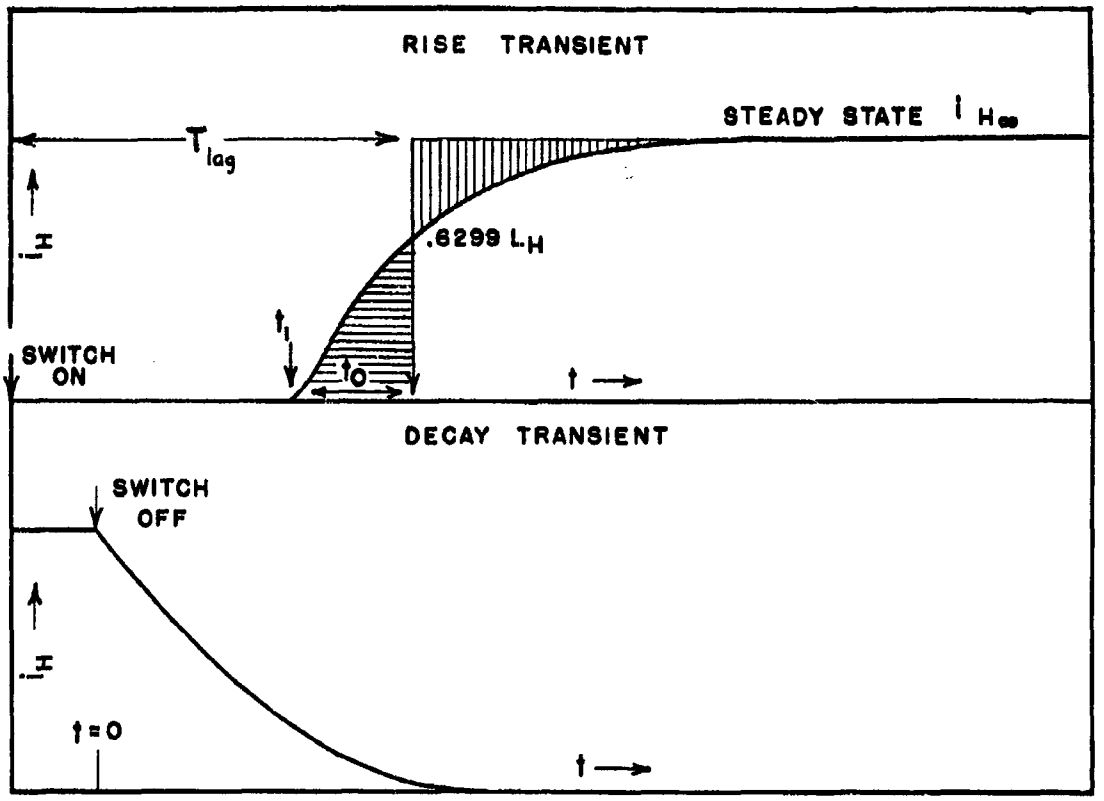
RISE TRANSIENT
STEADY STATE $I_{H\infty}$
T_{lag}
I_H
.6299 $I_{H\infty}$
t_1
t_0
SWITCH ON
$t \rightarrow$
DECAY TRANSIENT
SWITCH OFF
I_H
$t=0$
$t \rightarrow$

FIG. 13

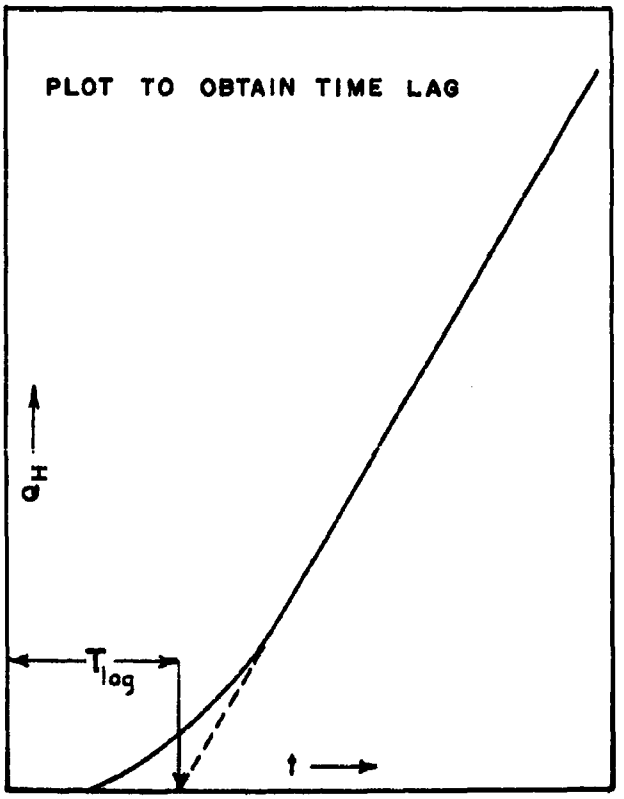
PLOT TO OBTAIN TIME LAG
σ_H
T_{lag}
$t \rightarrow$

FIG. 12

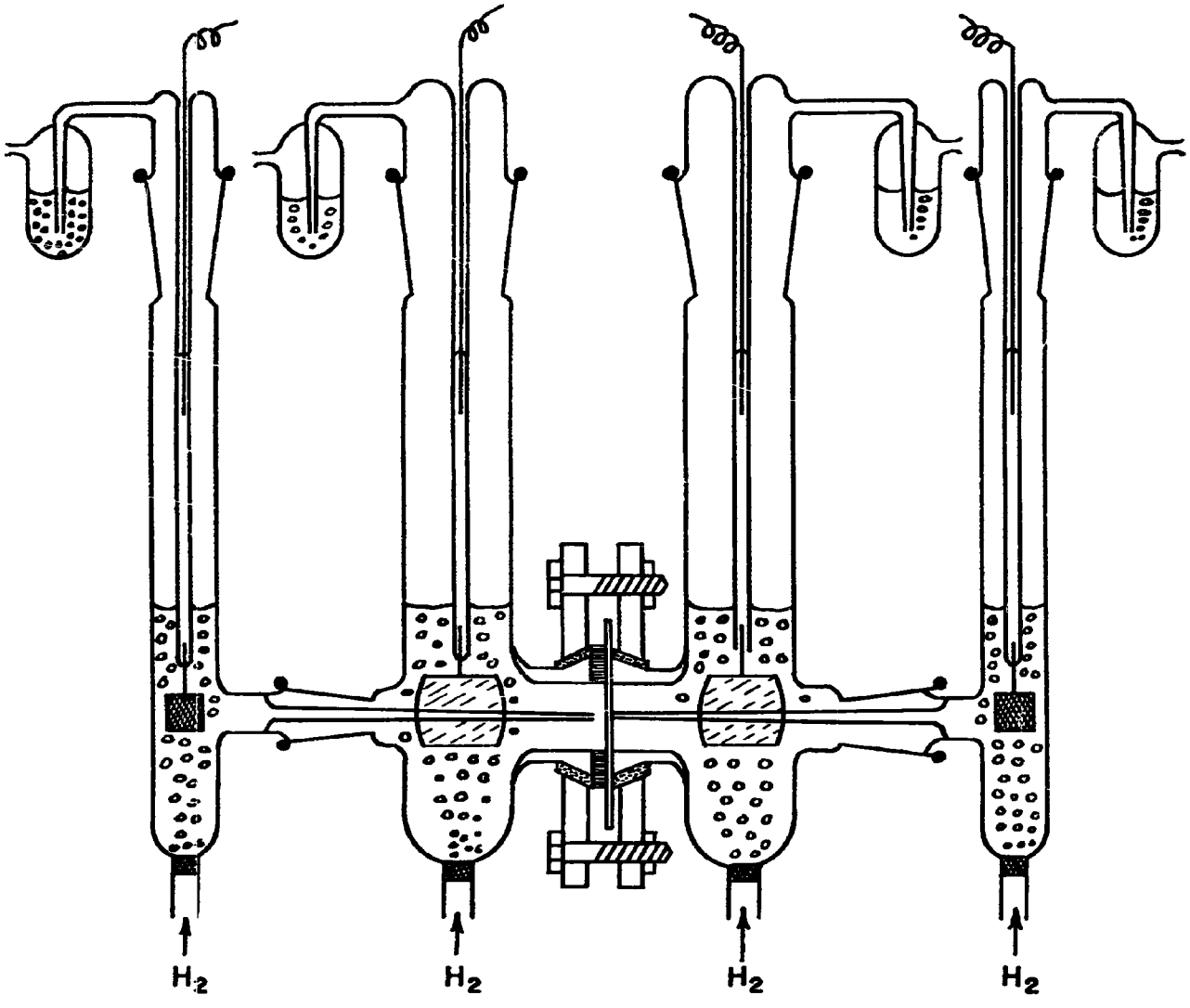

FIG. 14a

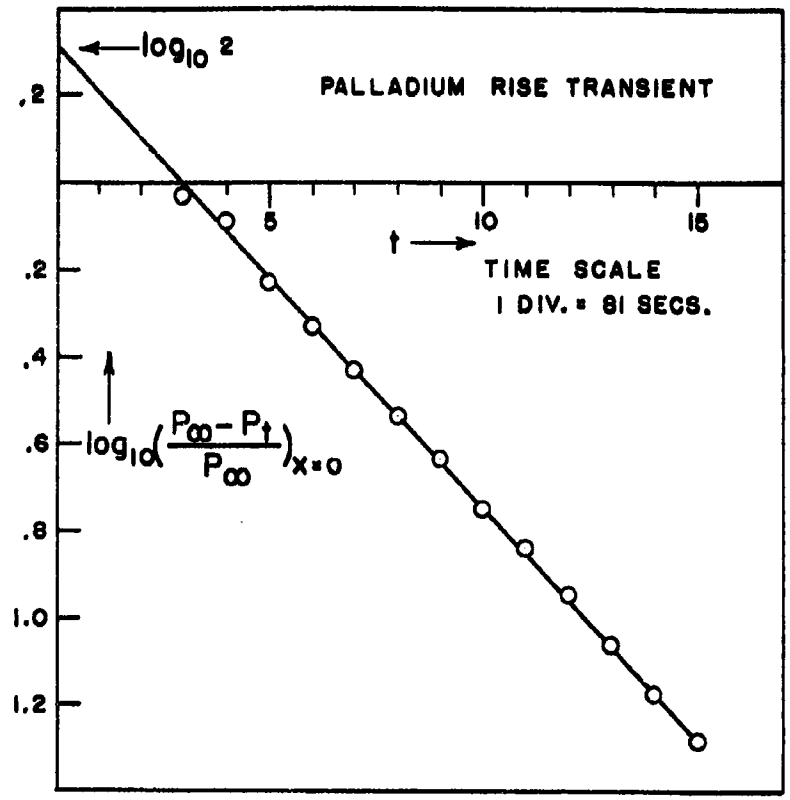
$\log_{10} 2$
PALLADIUM RISE TRANSIENT
.2
5
10
15
t
TIME SCALE
1 DIV. = 81 SECS.
.2
.4
.6
.8
1.0
1.2
$\log_{10}\left(\frac{P_\infty - P_t}{P_\infty}\right)_{x=0}$

FIG. 15

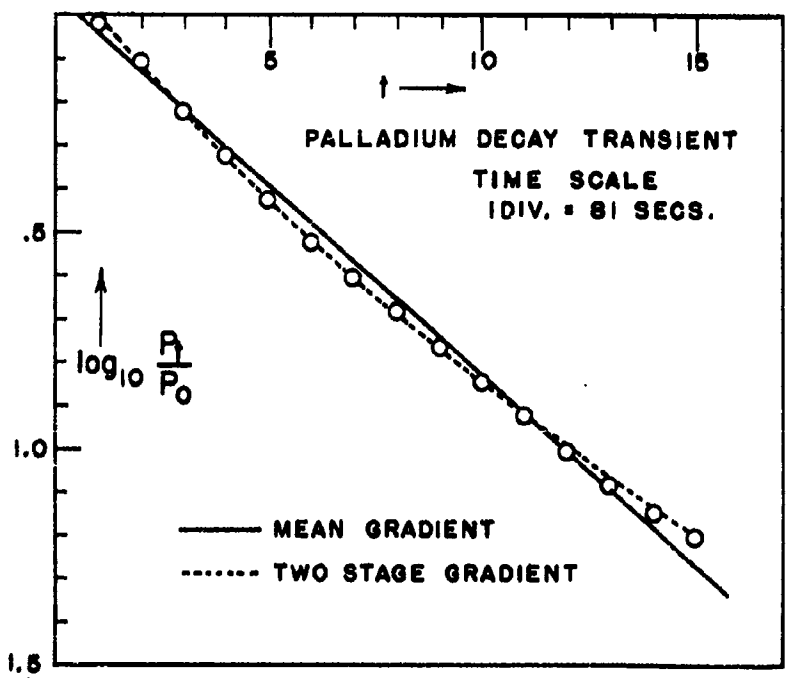
5
10
15
t
PALLADIUM DECAY TRANSIENT
TIME SCALE
1DIV. = 81 SECS.
.5
1.0
1.5
$\log_{10} \frac{P_t}{P_0}$
MEAN GRADIENT
TWO STAGE GRADIENT

FIG. 16

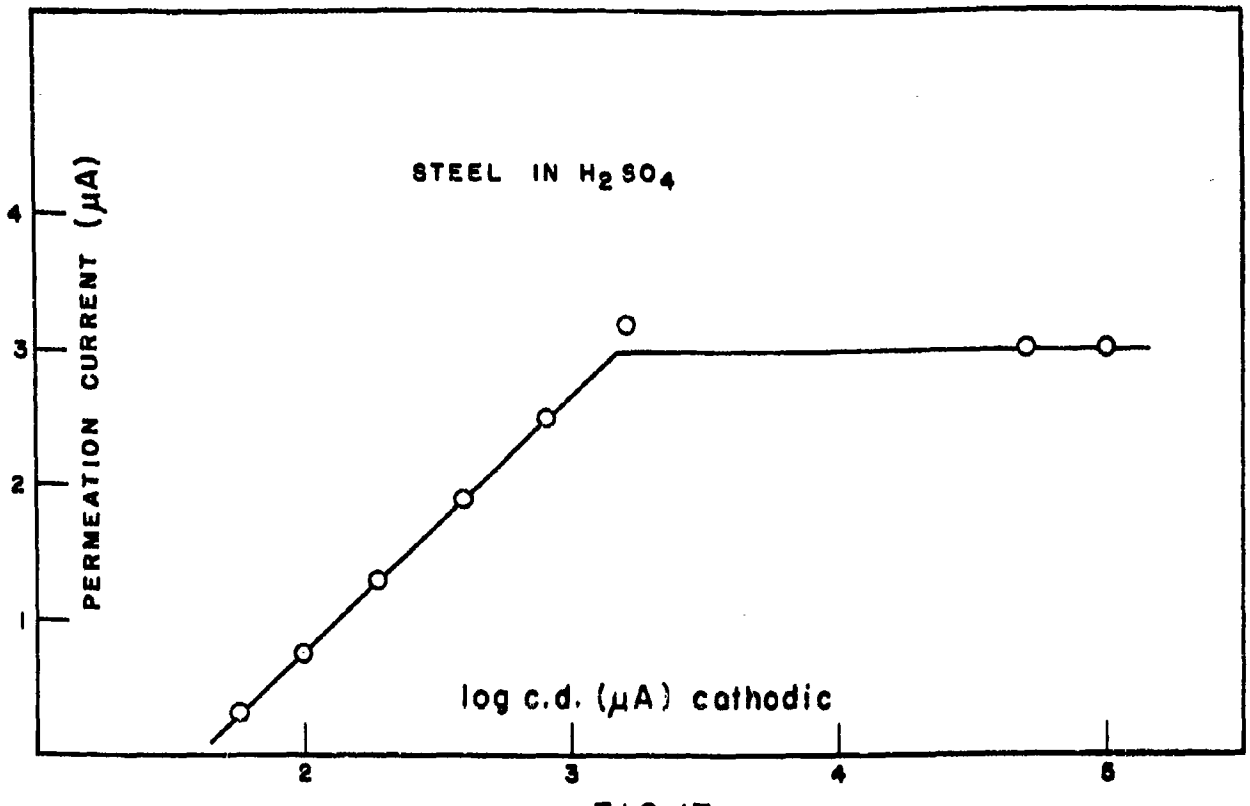
STEEL IN H_2SO_4
PERMEATION CURRENT (μA)
4
3
2
1
log c.d. (μA) cathodic
2
3
4
5

FIG. 17

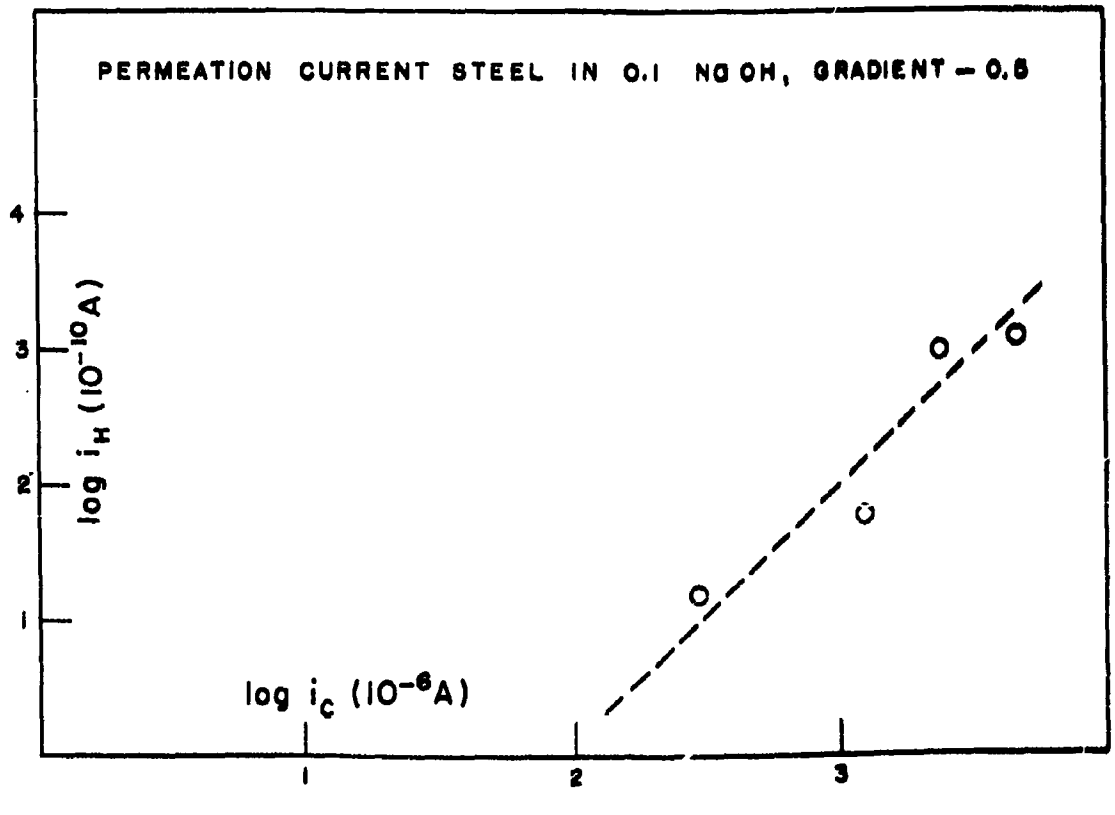
PERMEATION CURRENT STEEL IN 0.1 NaOH, GRADIENT – 0.8
log i_H (10^{-10}A)
4
3
2
1
log i_c (10^{-6}A)
1
2
3

FIG. 18

UNCLASSIFIED